QM/MM Study of the Reaction Catalyzed by Alkyladenine DNA Glycosylase: Examination of the Substrate Specificity of a DNA Repair Enzyme

Stefan A. P. Lenz and Stacey D. Wetmore*

Department of Chemistry and Biochemistry, University of Lethbridge, 4401 University Drive West, Lethbridge, Alberta T1K 3M4, Canada

SUPPORTING INFORMATION

(13 Pages)

Table S1. Summary of clustered MD simulations of AAG bound to DNA-containing Hx, G, or 7MeG. [a,b]

	Cluster	Occupancy	Avg Distance (σ)[c]	Avg Cluster Distance[d]
Hx	1	97.6%	0.544 (0.107)	0.818
	2	2.3%	0.594 (0.122)	0.846
	3	0.1%	0.487 (0.101)	0.885
G	1	95.8%	0.606 (0.105)	0.897
	2	2.7%	0.521 (0.103)	0.874
	3	0.7%	0.587 (0.124)	0.929
7MeG	1	93.7%	0.517 (0.102)	0.837
	2	6.2%	0.436 (0.069)	0.882
	3	0.1%	0.567 (0.056)	0.913

[a]Each trajectory was clustered according to the positions of the bound nucleotide and active site residues (E125, Y127, A135, H136, Y159, and N169) using a hierarchical agglomerative average linkage rmsd algorithm. [b]Final production simulations were taken from reference 41 in the main text. [c]Average distance (Å) between each point within a cluster. [d]Average distance (Å) between each cluster.

Table S2. Deviations in calculated position of active site residues (rmsd, Å) when AAG is bound to Hx, G, or 7MeG using different ONIOM(QM:MM) methodologies.

Bound Nucleotide	Stationary Point	Calculation Method		rmsd[a]
Hx	RC	Constrained B3LYP[b]	Constrained B3LYP-D3[c]	0.134
Hx	TS	Constrained B3LYP[b]	Constrained B3LYP-D3[c]	0.141
Hx	PC	Constrained B3LYP[b]	Constrained B3LYP-D3[c]	0.143
Hx	RC	Unconstrained B3LYP-D3[d]	Constrained B3LYP-D3[c]	0.010
Hx	TS	Unconstrained B3LYP-D3[d]	Constrained B3LYP-D3[c]	0.025
Hx	PC	Unconstrained B3LYP-D3[d]	Constrained B3LYP-D3[c]	0.164
G	RC	Constrained B3LYP[b]	Constrained B3LYP-D3[c]	0.170
G	RC	Unconstrained B3LYP-D3[d]	Constrained B3LYP[b]	0.188
G	RC	Unconstrained B3LYP-D3[d]	Constrained B3LYP-D3[c]	0.037
7MeG	RC	Constrained B3LYP[b]	Constrained B3LYP-D3[c]	0.151
7MeG	$TS_{dissociative}$	Constrained B3LYP[b]	Constrained B3LYP-D3[c]	0.278
7MeG	IC	Constrained B3LYP[b]	Constrained B3LYP-D3[c]	0.162
7MeG	$TS_{associative}$	Constrained B3LYP[b]	Constrained B3LYP-D3[c]	0.179
7MeG	PC	Constrained B3LYP[b]	Constrained B3LYP-D3[c]	0.213
7MeG	$TS_{concerted}$	Constrained B3LYP[b]	Constrained B3LYP-D3[c]	0.221

[a]rmsd (Å) of active site residues in the QM layer (including the bound nucleotide, E125, Y127, A135, H136, Y159, and N169). [b]Constrained ONIOM(B3LYP/6-31G(d):AMBER) stationary points. [c]Constrained ONIOM(B3LYP-D3/6-31G(d):AMBER) stationary points. [d]Unconstrained ONIOM(B3LYP-D3/6-31G(d):AMBER) stationary points.

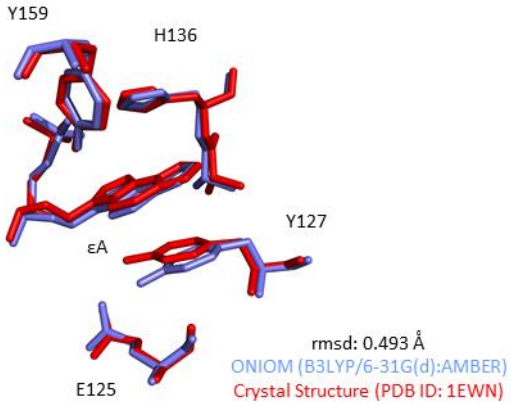

Figure S1. Overlay of the X-ray crystal structure of AAG bound to DNA-containing εA (red, see reference 34) and corresponding complex optimized with ONIOM(B3LYP/6-31G(d):AMBER) (blue).

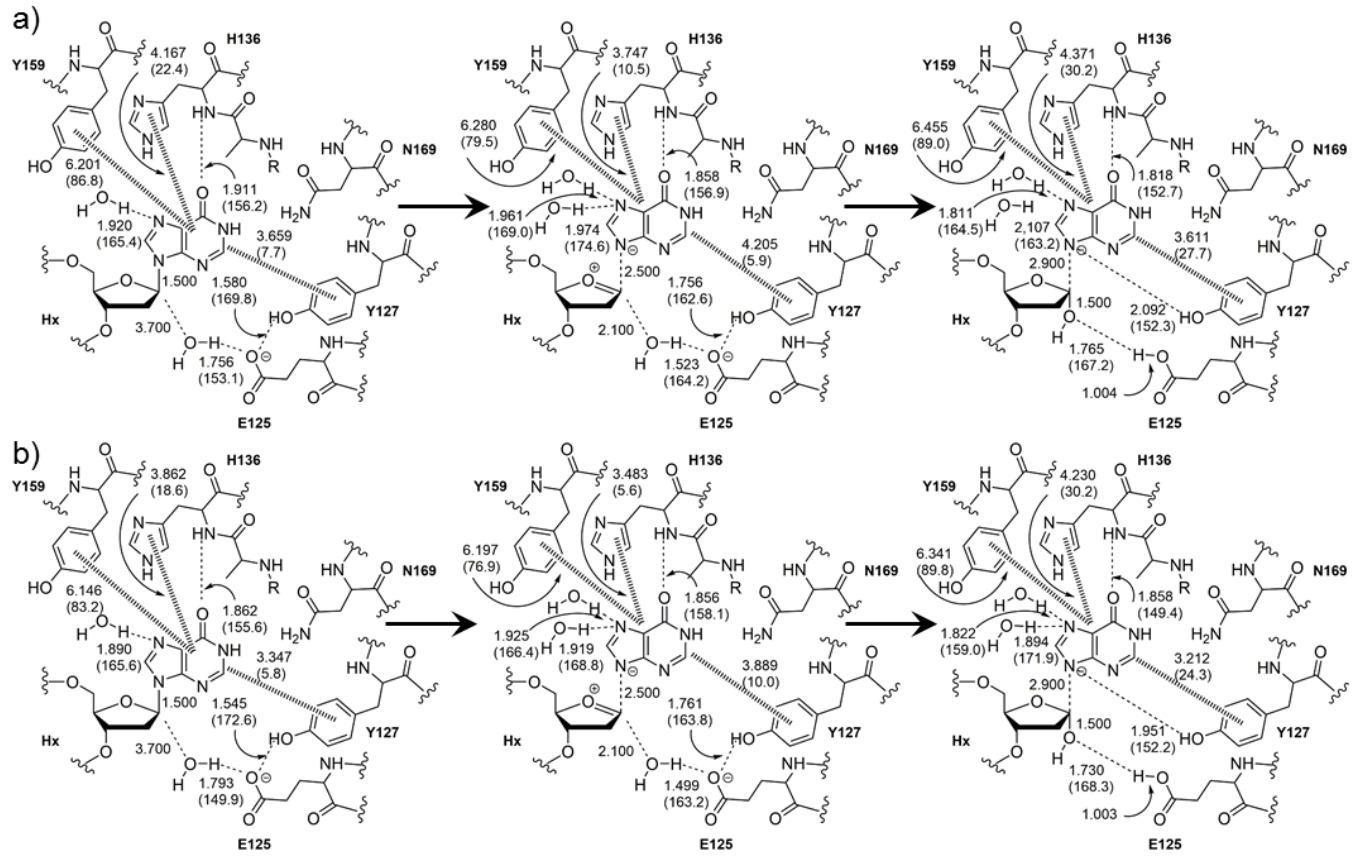

Figure S2. Structures of constrained a) ONIOM(B3LYP/6-31G(d):AMBER) and b) ONIOM(B3LYP-D3/6-31G(d):AMBER) stationary points (RC, TS, and PC) corresponding to AAG-mediated excision of Hx displayed as line diagrams, with distances in Å, angles in deg, and hashed bonds denoting π–π stacking or T-shaped interactions.

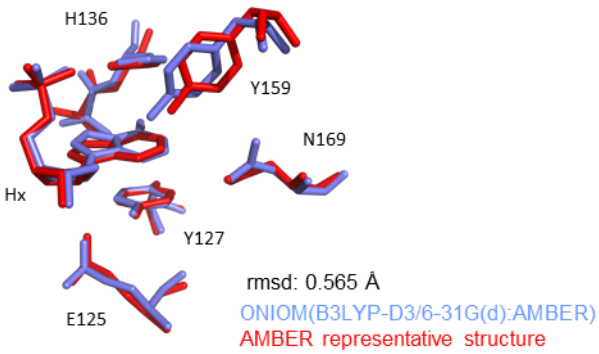

Figure S3. Overlay of the unconstrained ONIOM(B3LYP-D3/6-31G(d):AMBER) RC (blue) and representative MD (AMBER) structure (red) of Hx bound in the AAG active site.

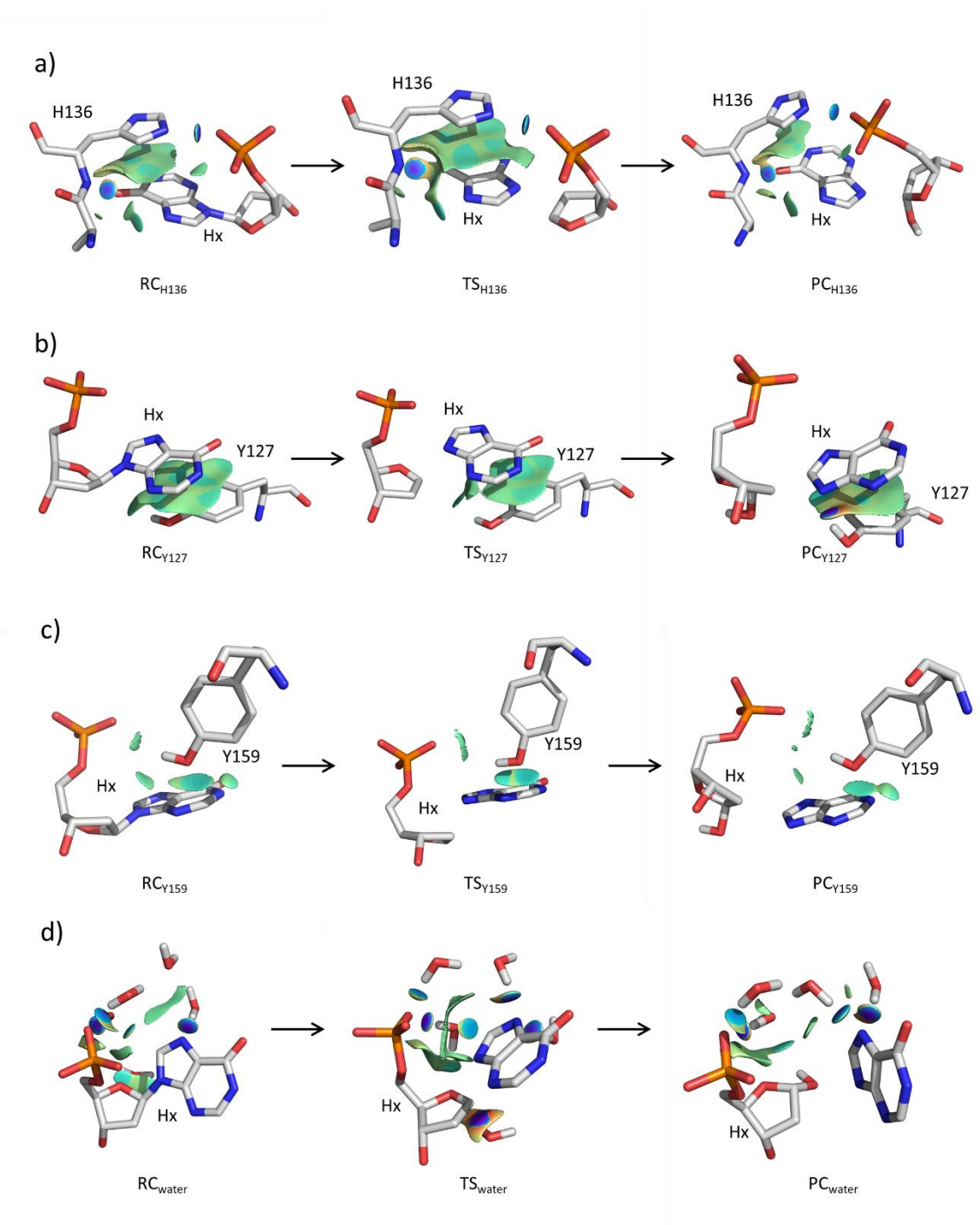

Figure S4. NCI plots depicting interactions between the nucleotide and a) H136, b) Y127, c) Y159, or d) water along the AAG-mediated excision of Hx. Promolecular densities are reported when the reduced density gradient is less than or equal to 0.3 and the color ranges from –0.0500 au (attractive interaction) to +0.0500 au (repulsive interaction).

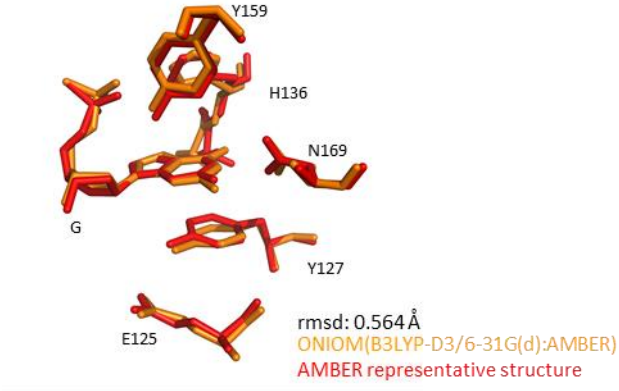

Figure S5. Overlay of the constrained ONIOM(B3LYP-D3/6-31G(d):AMBER) RC (orange) and representative MD (AMBER) structure (red) of G bound in the AAG active site.

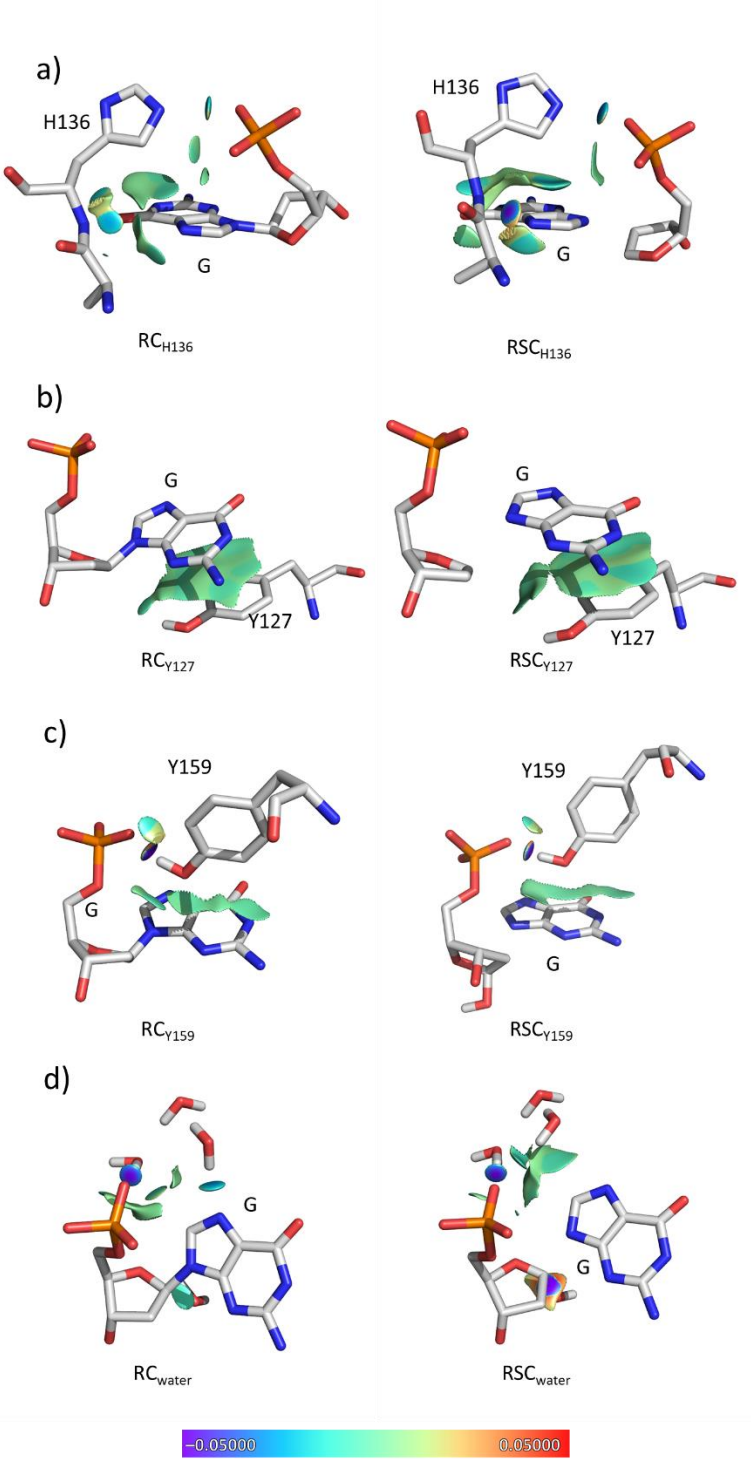

Figure S6. NCI plot depicting interactions between the nucleotide and a) H136, b) Y127, c) Y159, or d) water for the G reactant complex (RC) and representative structure with an elongated glycosidic bond obtained from the G reaction surface (denoted RSC). Promolecular densities are reported when the reduced density gradient is less than or equal to 0.3 and the color ranges from –0.0500 au (attractive interaction) to +0.0500 au (repulsive interaction).

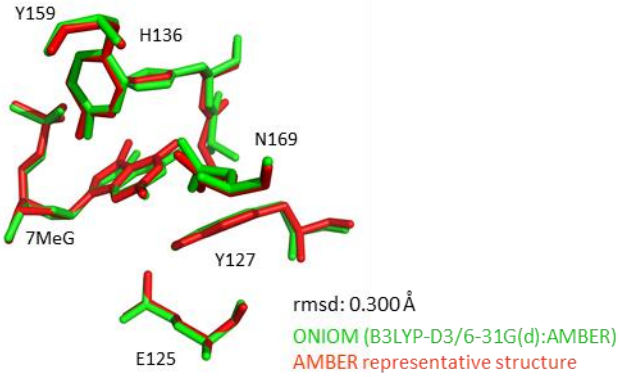

Figure S7. Overlay of the constrained ONIOM(B3LYP-D3/6-31G(d):AMBER) RC (green) and representative MD (AMBER) structure (red) of 7MeG bound in the AAG active site.

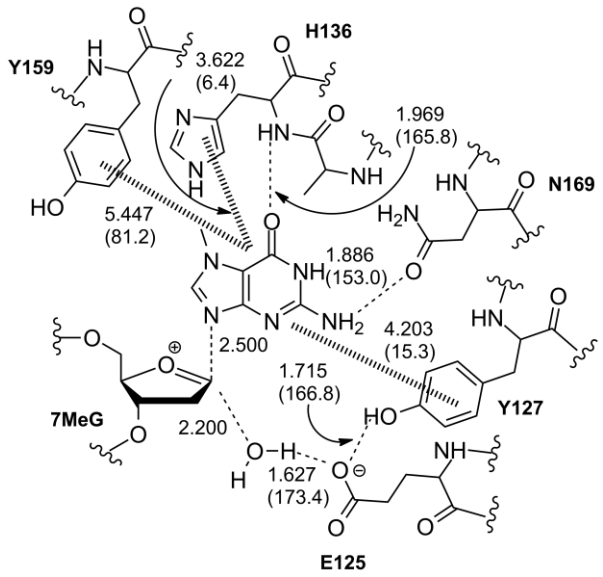

Figure S8. Structures of constrained ONIOM(B3LYP-D3/6-31G(d):AMBER) concerted TS corresponding to AAG-mediated excision of 7MeG displayed as a line diagram, with distances in Å, angles in deg, and hashed bonds denoting π–π stacking or T-shaped interactions.

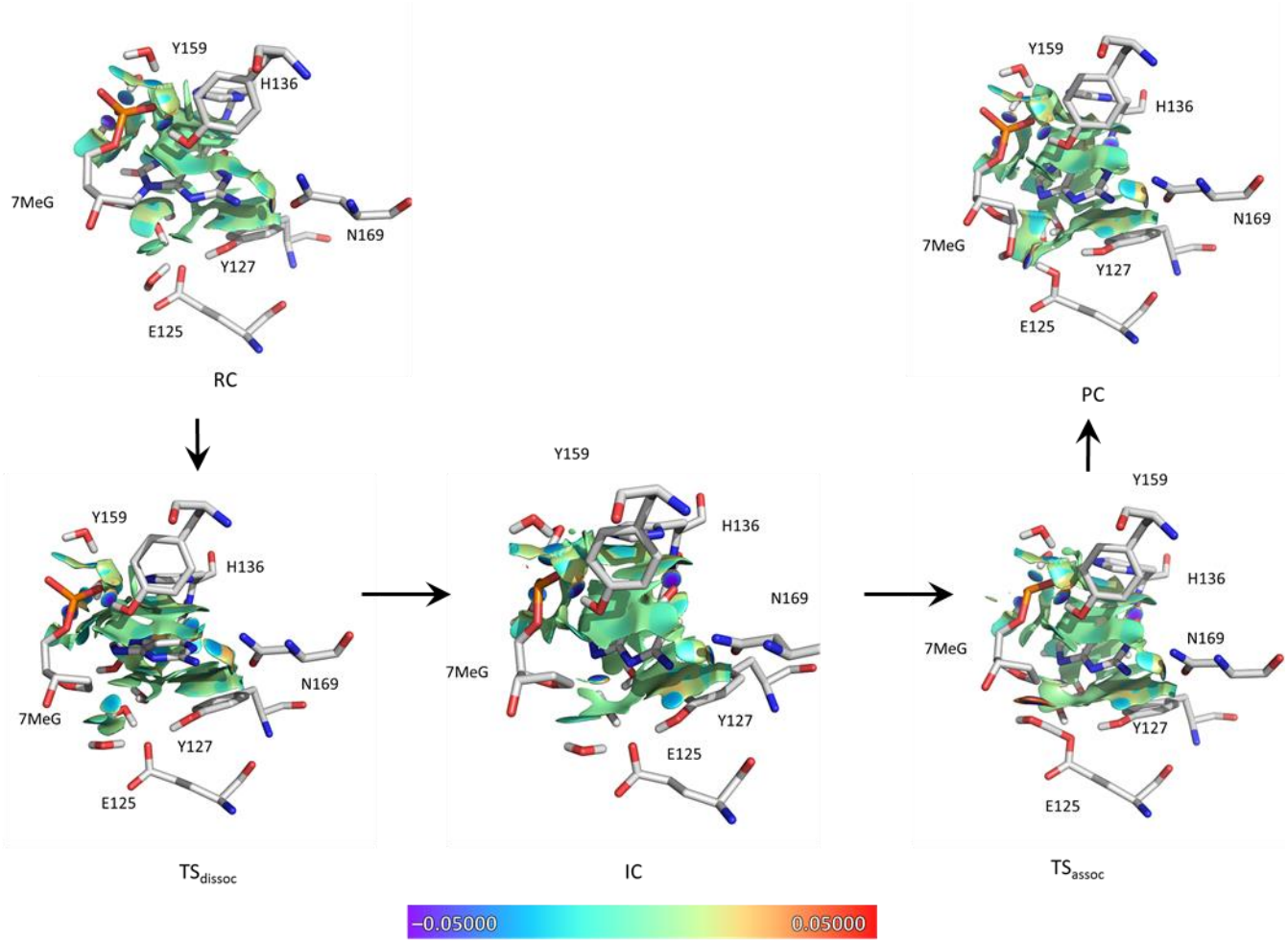

Figure S9. NCI plots of the constrained ONIOM(B3LYP-D3/6-31G(d):AMBER) stationary points (RC, TS_{dissoc}, IC, TS_{assoc} and PC) corresponding to AAG-mediated excision of 7MeG. Promolecular densities are reported when the reduced density gradient is less than or equal to 0.3 and the color ranges from –0.0500 au (attractive interaction) to +0.0500 au (repulsive interaction).

Full citations for references 68 and 74

[68] Case, D. A., Darden, T. A., Cheatham, T. E., III, Simmerling, C. L., Wang, J., Duke, R. E., Luo, R., Crowley, M., Walker, R. C., Zhang, W., Merz, K. M., Wang, B., Hayik, S., Roitberg, A., Seabra, G., Kolossvary, I., Wong, K. F., Paesani, F., Vanicek, J., Wu, X., Brozell, S. R., Steinbrecher, T., Gohlke, H., Yang, L., Tan, C., Mongan, J., Hornak, V., Cui, G., Mathews, D. H., Seetin, M. G., Sagui, C., Babin, V., and Kollman, P. A. (2008) AMBER Tools, Version 1.0 ed., University of California, San Francisco.

[74] Frisch, M. J.; Trucks, G. W.; Schlegel, H. B.; Scuseria, G. E.; Robb, M. A.; Cheeseman, J. R.; Scalmani, G.; Barone, V.; Mennucci, B.; Petersson, G. A.; Nakatsuji, H.; Caricato, M.; Li, X.; Hratchian, H. P.; Izmaylov, A. F.; Bloino, J.; Zheng, G.; Sonnenberg, J. L.; Hada, M.; Ehara, M.; Toyota, K.; Fukuda, R.; Hasegawa, J.; Ishida, M.; Nakajima, T.; Honda, Y.; Kitao, O.; Nakai, H.; Vreven, T.; Montgomery Jr., J. A.; Peralta, J. E.; Ogliaro, F.; Bearpark, M. J.; Heyd, J.; Brothers, E. N.; Kudin, K. N.; Staroverov, V. N.; Kobayashi, R.; Normand, J.; Raghavachari, K.; Rendell, A. P.; Burant, J. C.; Iyengar, S. S.; Tomasi, J.; Cossi, M.; Rega, N.; Millam, N. J.; Klene, M.; Knox, J. E.; Cross, J. B.; Bakken, V.; Adamo, C.; Jaramillo, J.; Gomperts, R.; Stratmann, R. E.; Yazyev, O.; Austin, A. J.; Cammi, R.; Pomelli, C.; Ochterski, J. W.; Martin, R. L.; Morokuma, K.; Zakrzewski, V. G.; Voth, G. A.; Salvador, P.; Dannenberg, J. J.; Dapprich, S.; Daniels, A. D.; Farkas, Ö.; Foresman, J. B.; Ortiz, J. V.; Cioslowski, J.; Fox, D. J. *Gaussian 09*, Revisions C.01 and D.01; Gaussian, Inc.: Wallingford, CT, USA, 2009.